

ENGINEERING RESEARCH INSTITUTE
THE UNIVERSITY OF MICHIGAN
ANN ARBOR

STATISTICAL THEORY OF THE
MAGNETRON SPACE CHARGE

By

Gunmar Hok

Approved by:


J. E. Rowe

Project 2275-2

CONTRACT NO. DA-36-039 sc 56714
SIGNAL CORPS, DEPARTMENT OF THE ARMY
DEPARTMENT OF THE ARMY PROJECT NO. 3-30-06-032
SIGNAL CORPS PROJECT NO. 1143A
PLACED BY THE U. S. ARMY SIGNAL CORPS
ENGINEERING LABORATORIES
FORT MONMOUTH, NEW JERSEY

February, 1958

Engu

AMR

2039

TABLE OF CONTENTS

ABSTRACT	iv
LIST OF ILLUSTRATIONS	v
INTRODUCTION	1
PHASE-SPACE DESCRIPTION OF THE SPACE-CHARGE DISTRIBUTION	2
APPROXIMATE DETERMINATION OF THE SPACE-CHARGE DISTRIBUTION	8
CONFIRMATION AND CONCLUSION	18
APPENDIX--CALCULATION OF THE DENSITY IN THE SECULAR REGION	23
LIST OF REFERENCES	27

ABSTRACT

The general conclusions regarding the space-charge distribution in a cutoff magnetron which were first presented in the Technical Report No. 10 have now been very well established by experimental observations. The report submitted here develops the statistical theory quantitatively by successive approximations. A first-order approximation of the distribution in phase space is obtained in closed form. A nonphysical singularity in this distribution is eliminated in the second-order distribution, which requires rough approximations or numerical methods for its solution. A qualitative discussion of the second-order distribution and a comparison with available experimental data are included.

In addition, an idealized approximation is discussed which is an intuitively more satisfactory basis for a small-signal theory than the Brillouin distribution.

The important conclusions are (1) that the space charge in the nonoscillating magnetron extends continuously to the anode and (2) that the radial distribution is not very different from that of an oscillating magnetron at small or moderate amplitudes of oscillation.

LIST OF ILLUSTRATIONS

<u>Figure</u>		<u>Page</u>
1	Mapping of Regions in Phase Space Accessible to Electrons Whose Orbits Intersect the Anode or the Cathode Plane.	5
2	Mapping of the Secular Region in Phase Space for the First-Order Calculations.	12
3	Volume-Preserving Transformation of the First-Order Secular Region.	13
4	Samples of Space Charge Along the Axis of the Secular Region.	16
5	Shape of the Secular Region in the Second Approximation.	17
6	Observed Density of Electrons of More Than 20 Electron Volts Energy in a Static Magnetron (Nedderman).	20
7	Comparison of Nedderman's Results for Different Values of the Magnetic Field.	21

STATISTICAL THEORY OF THE MAGNETRON SPACE CHARGE

I. Introduction

The space charge in an electron tube is essentially a dilute gas formed by discrete electrons. Theoretical models for the behavior of such space charge may therefore be borrowed from classical statistical mechanics. However, in most tubes the "life time" or transit time of an electron between electrodes is so short that simpler models suffice to give an adequate description. The most powerful tools of statistical mechanics are available and helpful primarily for the analysis of systems in or approaching thermodynamic equilibrium.

The state of a cut-off magnetron comes closer to such an equilibrium than most electron configurations in vacuum tubes. There is evidence that a sizeable fraction of the electrons remain in the gas for periods of time that are extremely long compared to the time of flight, say, from the cathode or potential minimum to a point as close to the anode as the magnetic field permits, and back again. Under these circumstances even very weak interaction between the electrons may radically modify the distribution of the electron gas in the space between anode and cathode. The steady-state distribution will be approached more slowly, if the interaction or random fluctuations of potential are extremely small, but until this state is reached, the distribution must drift towards it.

Statistical mechanics offers a convenient language for the discussion and qualitative description of this problem, even if a complete

quantitative solution may appear extremely difficult. Once the problem is approached from this point of view, it becomes immediately clear that the various space-charge distributions originally proposed have very low entropy and are extremely unlikely ever to occur in an actual tube, except possibly as highly transient states.

II. Phase-Space Description of the Space-Charge Distribution

In a magnetic field of the flux density $B = \text{curl } A$, the generalized momentum of an electron of mass m and charge $-q_e$ is defined as the vector

$$p = mu - q_e A \quad (1)$$

if the electron is moving with velocity u .

The nonrelativistic energy of the electron in an electric field of the scalar potential V is then

$$W = \frac{1}{2} mu^2 - q_e V = \frac{1}{2m} \left[p + q_e A \right]^2 - q_e V \quad (2)$$

Let us consider a plane magnetron with its cathode plane at $y = 0$ and anode at $y = d$; the uniform magnetic flux density directed along the positive z -axis may be represented by a vector potential

$$A = By \quad (3)$$

parallel to the x -axis. If for the moment conservation of energy and momentum is assumed along the orbit of an electron in the magnetron, the electron "energy state" may be said to be completely specified by the components p_x, p_z and its energy W . These are the "constants of the motion," while the potential energy $-q_e V$ and the momentum component p_y vary along the orbit. Actually, the conservation laws do not hold for each electron individually; close encounters between electrons and small

fluctuations of the potential perturb the orbits and may be said to produce transitions from one energy state to another.

The simplicity of the plane configuration may be maintained and still the dimensions kept finite by the conventional trick of cyclic boundary conditions. An electron leaving in the positive x-direction may be thought of as reappearing from the negative x-direction; the same rule may be applied to the z-dimension.

The space-charge distribution and dynamics may be described by the electron density in phase space or μ -space, i.e. the six-dimensional space with the coordinates $x, y, z, p_x, p_y,$ and p_z . For the purpose of the present analysis a subspace y, p_x, p_y will permit the study of all the essential phenomena and boundary surfaces of the problem.

Each energy state is represented by an orbit in a yp_y -plane of this space. Only one such curve is associated with each point.

For any given potential distribution $V(y)$ the regions in phase space directly accessible to electrons emitted from the cathode can be mapped. Equation (2) may be written

$$2mW = p_x^2 + p_{y0}^2 + p_z^2 = (p_x + q_e B y)^2 + p_y^2 + p_z^2 - 2mq_e V \quad (3)$$

where p_{y0} is the y-component of the electron momentum at the moment it crosses the plane $y = 0$. This equation may conveniently be written in dimensionless form by dividing y by the anode-cathode distance d , the momentum by $q_e B d$, and the potential by the cutoff voltage

$$V_c = \frac{q_e B^2 d^2}{2m} \quad (4)$$

giving the result

$$p_x^2 + p_{y0}^2 + p_z^2 = (p_x + y)^2 + p_y^2 + p_z^2 - V. \quad (5)$$

All points in phase space that satisfy this equation with a real

positive or zero value of p_{y0}^2 are accessible to electrons from the cathode emitted with the required momentum. Rearranging the terms we obtain

$$0 \leq p_{y0}^2 = p_y^2 + y^2 - V + 2p_x y \quad (6)$$

The equality sign gives the equation for the boundary surface of the accessible region. For constant y this equation represents a parabola in a $p_x p_y$ -plane. In the plane $p_y = 0$ the boundary is defined by the relation

$$p_x \geq \frac{1}{2} \left(\frac{V(y)}{y} - y \right) \quad (7)$$

Similarly a region can be specified for which all electron orbits intersect the anode plane $y = 1$. The corresponding equations are

$$0 \leq p_{ya}^2 = p_y^2 + y^2 - 1 - V + V_a + 2p_x(y - 1) \quad (8)$$

$$p_x \leq \frac{-(1 - y^2) + V_a - V}{2(1 - y)} = \frac{1}{2} \left[\frac{V_a - V}{1 - y} - (y + 1) \right] \quad (9)$$

These boundaries are shown qualitatively in Fig. 1. The solid lines refer to the cathode-accessible region, the broken lines to the anode-accessible region.

The shape of the region inaccessible from the cathode is that of a distorted cone with its apex on the p_x -axis, which is a generatrix of the surface. This does not mean that electrons on this part of the axis cannot escape from the cathode; they do, tangentially to the $p_x p_y$ -plane, and describe something like an elliptic orbit in a $y p_y$ -plane on the surface of the cone. The orbit that reaches the anode forms the intersection between the boundaries of the cathode-accessible and anode-accessible regions. It is the base plane of a distorted double cone, one apex of which is on the line $y = 0, p_y = 0$, the other on the line $y = 1, p_y = 0$.

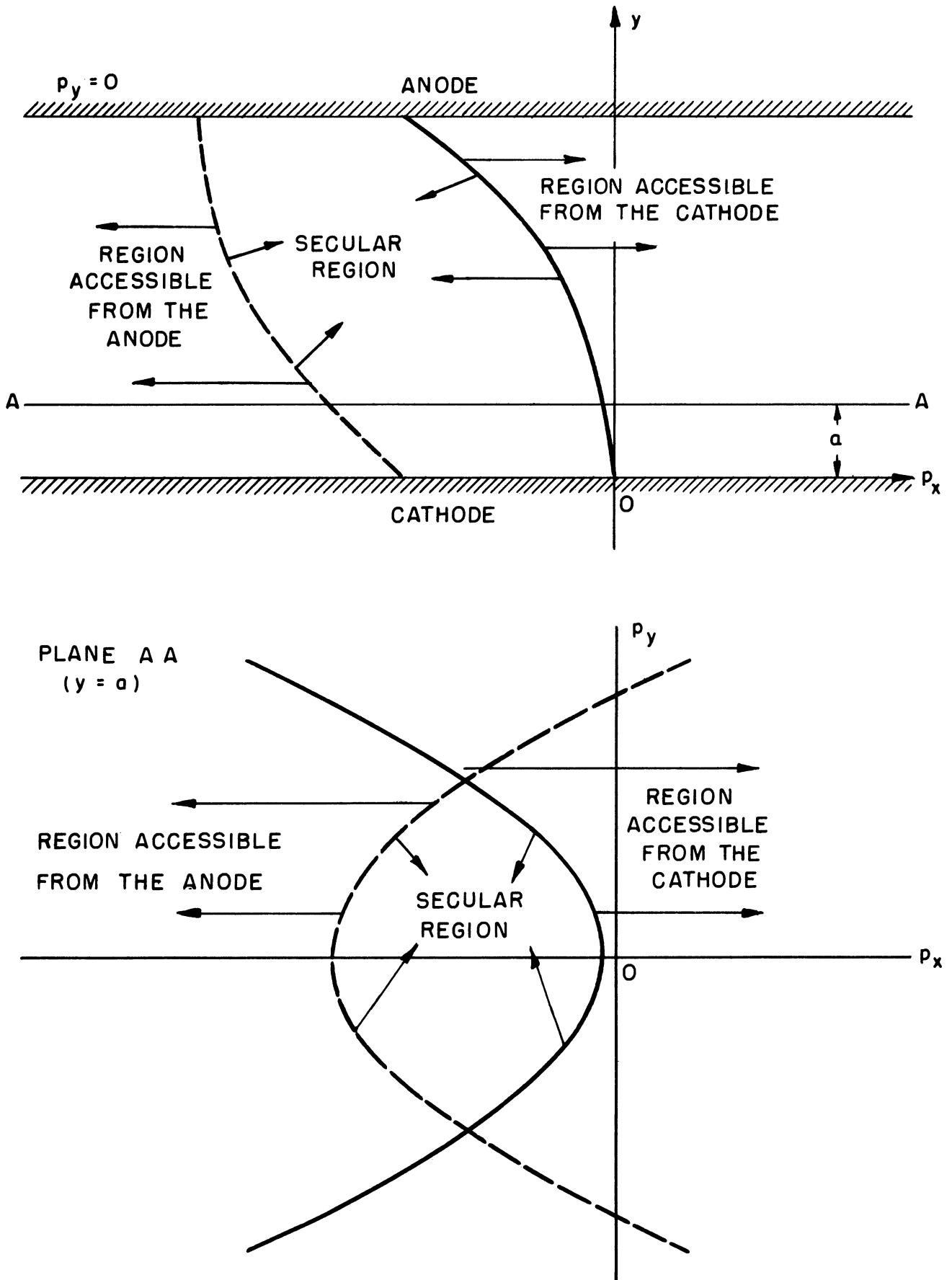


FIG. 1 MAPPING OF REGIONS IN PHASE SPACE ACCESSIBLE TO ELECTRONS WHOSE ORBITS INTERSECT THE ANODE OR THE CATHODE PLANE.

If the cathode is a good emitter operating under space-charge-limited conditions, the region between the cathode and the potential minimum will be in an approximate equilibrium just as in any diode at current densities far below saturation. We shall set $y = 0$ at the potential minimum rather than at the cathode and assume that the space-charge density automatically adjusts itself for zero potential gradient at this point.

The population in the cathode-accessible region is determined by the Maxwell-Boltzmann distribution at the potential minimum. The population of the anode-accessible region is virtually zero, since the anode does not emit electrons, and any electron appearing there will be captured by the anode in less than one orbital period.

Between these two regions there is a volume characterized by the fact that electrons may remain there for very long periods of time. Consequently, as long as there exists any process whatsoever by which momentum can be transferred between electrons in a random fashion, this "secular region" will gradually fill up with electrons until the density reaches a point where the outflux back to the cathode-accessible region and forward to the anode-accessible region equals the influx from the cathode region. When this condition is attained, a stable state has been established. This secular space charge, the existence of which has been experimentally confirmed, has a decisive influence on the distribution of potential and charge in the cutoff magnetron. It is therefore desirable to find a mathematical model to describe the flow of electrons through the secular region, in order that these distributions may be understood and predicted. We shall attempt to do this in a subsequent section.

In an electron gas the exchange of momentum between particles is

appreciably different from the corresponding process in an ideal gas formed by neutral molecules of relatively large cross sections. In the neutral gas two-body collisions constitute the predominant mechanism. In the electron gas two-body and three-body interaction may also produce appreciable momentum changes but only rather infrequently. The electric field of each electron, however, extends far beyond the effective collision cross section, and the sum of the fields of all the electrons in random motion gives a fluctuating rather than a constant potential at each point in space. These fluctuations are extremely small but they are continuous and may have a cumulative effect on the orbit of an electron. Both these two processes contribute to the transitions that make the electrons drift into and through the secular region. The transition probabilities depend in both instances on the population of the volume elements in phase space rather than on the difference in potential. The drift is consequently in a certain sense a diffusion process. The orbital convection currents that exist in the secular region are important factors in the establishment of the steady state, but they do not cross the boundaries. The drift of an electron through this region from one boundary to the opposite one can only take place through a long sequence of transitions from one energy state to another.

It is interesting to consider the phase-space distribution of the classical magnetron solutions. The single-stream Brillouin solution is concentrated into a single line along the y -axis in the (y, p_x, p_y) space (Fig. 1) from the origin to the Hull radius y_H . The lowest-order double-stream solution occupies a single, nearly elliptic orbit in the yp_y -plane, also confined to values of y smaller than y_H . These highly concentrated configurations have very low entropy, or in other words, are highly improbable in any physical multiparticle system that is left to itself for

any appreciable time. Mathematical models for the behavior of magnetrons based on such states may be useful for the prediction of physical phenomena only in limited areas, such as pulsed operation.

III. Approximate Determination of the Space-Charge Distribution

The suggestion that the current in a cutoff magnetron is produced by a process closely analogous to diffusion is the key to several approximate methods of evaluating the space-charge distribution. The justifications for this suggestion are

1. Only "transition current" (no "orbital current") crosses the boundaries of the secular region, which can easily be subdivided into compartments for which the same statement holds.

2. The momentum changes are isotropic, i.e., the transition probabilities are independent of sign and direction. Except at the anode and cathode, conservation of momentum holds for the gas as a whole, though not for each electron.

3. The infinitesimal momentum changes have by far the largest probability, so that nearly all transitions may be considered taking place between adjacent volume elements in phase space.

Under these conditions, the current is proportional to the concentration gradient parallel to the momentum axes in phase space. The detailed process by which the transitions take place, "preoscillations", potential fluctuations, etc., is immaterial, as long as it is compatible with these postulates. The space-charge distribution is independent of the "diffusion coefficient", which however determines the time required to establish a steady state and the amount of current flowing.

The simplest diffusion model of the cutoff magnetron is one-dimensional; the space-charge density falls linearly from the potential

minimum to zero at the anode. In the normalized variables this model is represented by the equations

$$-\rho = \frac{3}{2} V_a (1 - y) \quad (10)$$

$$V = \frac{1}{2} V_a (3y^2 - y^3), \quad (11)$$

or in dimensional variables

$$\rho = \frac{3V_a \epsilon_0}{d^3} (y - d), \quad (12)$$

$$V = \frac{V_a}{2d^3} (3dy^2 - y^3). \quad (13)$$

Although quantitatively a rather crude approximation, this model gives a much more realistic picture of the steady state of a nonoscillating magnetron than the Brillouin and the double-stream models. It is a single-stream model, and as such it is the steady-state counterpart of the transient Brillouin model. It implies that all the electrons drift through the secular region along the axis of the double cone. It is true that the density is a maximum there; nonetheless, this model is obviously an enormous oversimplification. There is actually a continuous distribution of well-populated elliptic orbits about the axis. Close to the electrodes a substantial fraction of the current is orbital, and consequently a smaller concentration gradient is required there to give the transition current necessary for continuity.

Closer approximations may be obtained by solving the diffusion problem in the three-dimensional phase space of Fig. 1. The solution may be obtained in four successive operations.

1. Calculate the boundaries of the secular region in phase space.
2. Set the electron density equal to zero at the boundaries of this region and find the "fundamental mode of diffusion" through the secular region, excited by a singular source at the apex of the cone.
3. Study the input boundary zone between the populated part of the cathode-accessible region and the secular region (i.e., nonsingular excitation).
4. Integrate the density over all momentum coordinates to obtain the density distribution in real space.

Self-consistency difficulties are involved, since the first operation requires knowledge of the potential distribution, which is available only after the fourth operation. A procedure of successive approximations may be followed, beginning with an assumed potential distribution. If the process converges reasonably fast, the result of the first cycle of operations may be accepted as an approximate solution.

The state represented by (10)-(11) offers itself as a natural zero-order approximation. However, in order to facilitate the second operation, we shall choose a constant charge density in real space

$$\rho = \rho_0 = -V_a \tag{14}$$

and

$$V = V_a y^2 . \tag{15}$$

The accessibility boundaries in the yp_x -plane are then, according to (7) and (9),

$$p_x = \frac{1}{2} y (V_a - 1) \quad (\text{from the cathode}) \quad (16)$$

and

$$p_x = \frac{1}{2} (y + 1) (V_a - 1) \quad (\text{to the anode}) . \quad (17)$$

In a plane of constant p_x the boundaries are in the same way found to be

$$p_y^2 + \left[y_1 + p_x (1 - V_a)^{-1/2} \right]^2 = p_x^2 (1 - V_a)^{-1} \quad (\text{cathode}) \quad (18)$$

and

$$p_y^2 + \left[y_1 + p_x (1 - V_a)^{-1/2} \right]^2 = (p_x + 1 - V_a)^2 (1 - V_a)^{-1} \quad (\text{anode}) . \quad (19)$$

Here the y -coordinate has been renormalized so as to make these boundaries and all the corresponding orbit projections circular:

$$y_1 = y(1 - V_a)^{1/2} . \quad (20)$$

In this momentum scale the distance between anode and cathode shrinks to zero as the cutoff voltage is approached.

Figure 2 shows the shape of secular region obtained by this simple model. The populated part of the cathode-accessible region enfolds the top of the secular region near the origin. Everywhere else the density must be zero along all the boundary surfaces.

Because of the circular orbital currents in the secular region, all circular volume elements in this region can be considered to have uniform density. For this reason an approximately equivalent double cone can be constructed, the axis of which is perpendicular to the orbital planes (Fig. 3). Since the altitude and base of the cone remain invariant under this transformation, the volume of the cone and of all circular volume elements are also

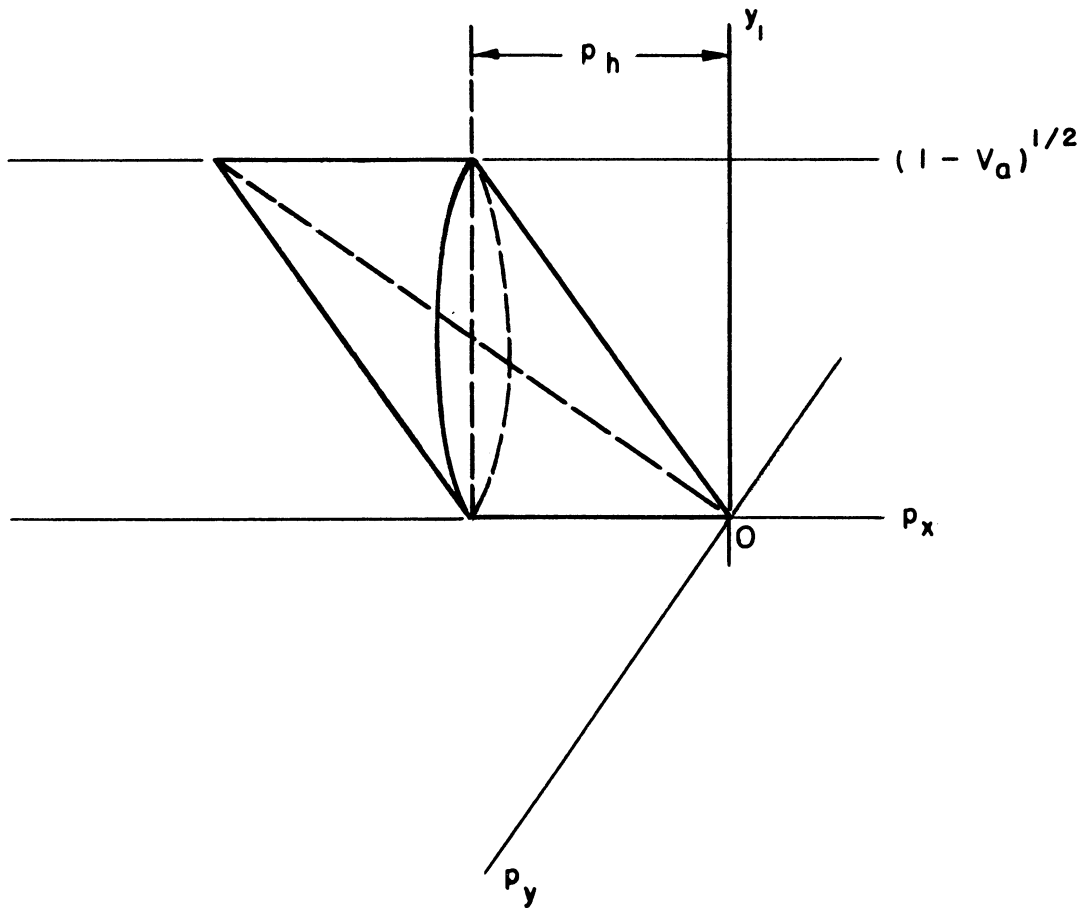


FIG. 2 MAPPING OF THE SECULAR REGION IN PHASE SPACE FOR THE FIRST-ORDER CALCULATIONS.

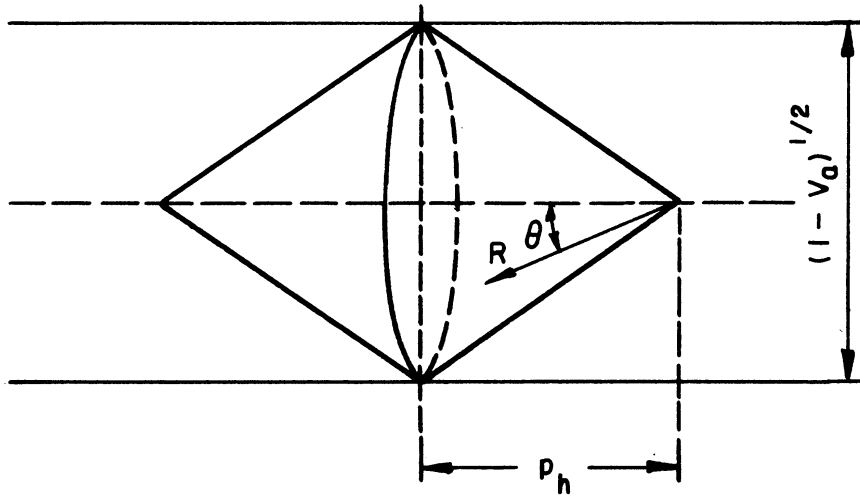


FIG. 3 VOLUME - PRESERVING TRANSFORMATION OF THE FIRST-ORDER SECULAR REGION.

invariant; so is the density of any volume element specified by its orbital radius and its altitude coordinate p_x . The diffusion from the apex of the right-hand cone is, with a slight modification, the solution of Laplace's equation in spherical coordinates (R, θ, ϕ) . The density does not vary with ϕ . The term representing diffusion in the θ -direction must be cut in half, because no primary diffusion takes place in the y -direction; any displacement in this dimension is orbital, subsequent to a change in momentum. The solution is

$$\rho = A \left\{ R^{\gamma_2} + \mu R^{\gamma_2} \right\} P_n(\cos \theta) \quad . \quad (21)$$

The order n of the Legendre function is such that its first zero occurs for the half-angle α of the cone

$$\theta_{no} = \alpha = \arctan(1 - V_a)^{-1/2} \quad . \quad (22)$$

Since $45^\circ < \alpha < 90^\circ$, n is between the limits $2.62 > n > 1$.

A and μ are constants determined by the radial boundary conditions.

If γ_2 is the larger exponent, the expression

$$\rho = BR_1^{\gamma_2} P_n(\cos \theta_1) \quad (24)$$

is the density in the left-hand cone referred to the spherical coordinate system centered on the apex to the left, where no source is located.

The fundamental diffusion modes described by (21) and (24) cannot be made to match with respect to density and gradient at the common base surface of the two cones; an infinite number of modes involving higher-order Legendre functions are required. However, an approximate result may be obtained by equating (21) and (24) on the axis ($\theta = \theta_1 = 0$) and neglecting the higher-order modes. The coefficients are found to be

$$\mu = \frac{1}{\gamma_2} p_h^{\gamma_2 - \gamma_1} \quad (25)$$

and

$$B = \left(\frac{1}{\gamma_2} + 1\right) p_h^{\gamma_2 - \gamma_1} \cdot A \quad (26)$$

where p_h is the altitude of each half of the double cone.

The approximate density in phase space is now known everywhere, except for the constant factor A. Integration with respect to p_x and p_y yields the density variation with y . After integration of Poisson's equation, this constant is obtained from the potential difference between the anode and the potential minimum.

Since the density is a maximum along the axis of the secular space, a significant sample of the space-charge distribution may now easily be obtained by calculating the charge in a narrow conical volume element in each cone. Projected on the y -axis this charge is shown in Fig. 4 for two different anode voltages. The final integration is roughly equivalent to scanning this plot by means of a rather broad aperture function.

The resulting first-order space-charge distribution differs considerably from the one originally assumed; in other words, the solution is still far from selfconsistent. The singularity at $y = 0$ is obviously non-physical. There are two circumstances that contribute to smoothing out the distribution close to the cathode. The apex of the cone is moved far towards positive p_x , so that the exciting Maxwell-Boltzmann distribution forms an annular source around the cone at $p_x = 0$. The second circumstance is the rapidly growing flaring angle of the "cone" in the direction toward its base plane (Fig. 5). The first point is most important close to cutoff; the second becomes particularly significant far from cutoff. The orbits

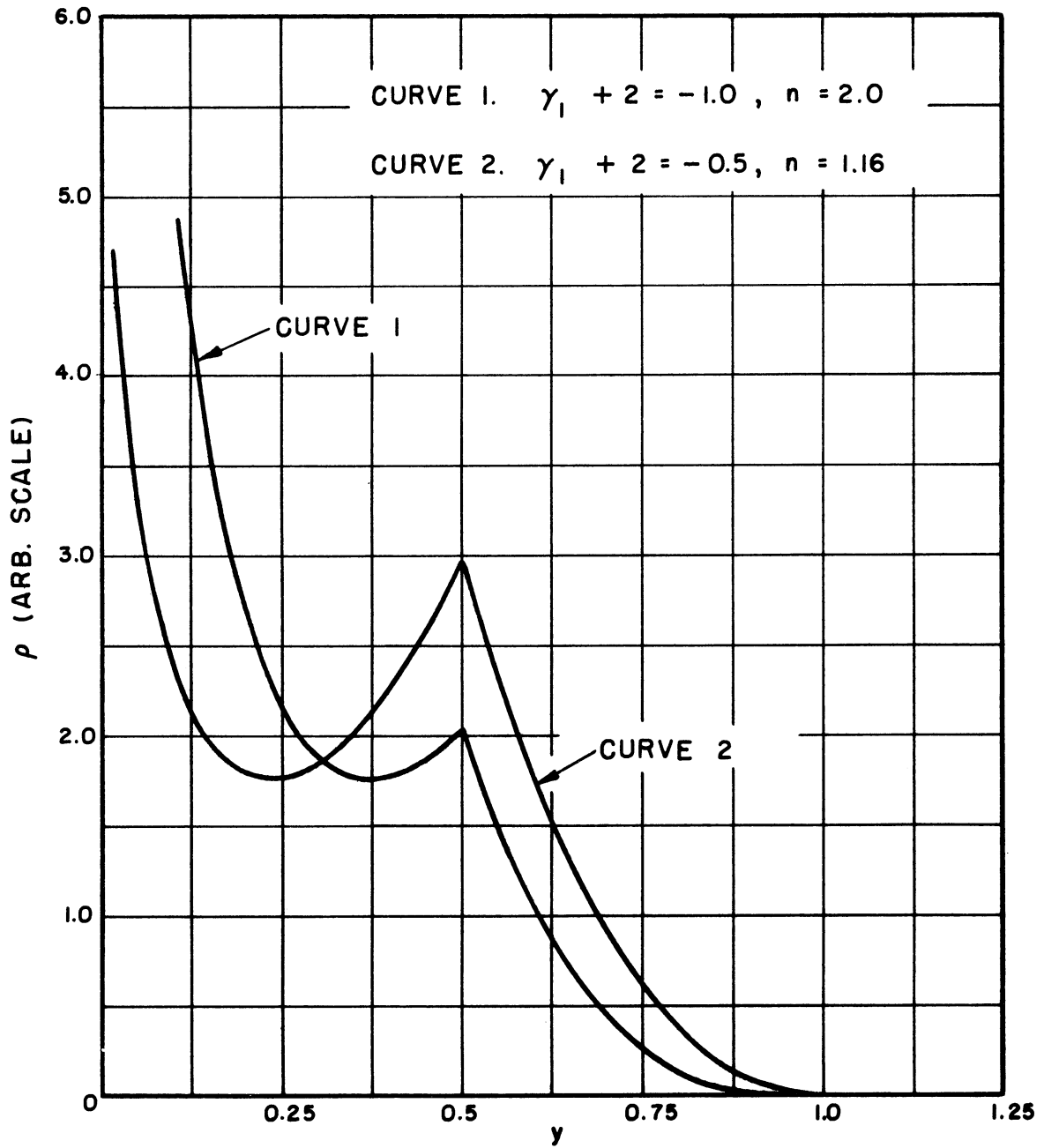


FIG. 4 SAMPLES OF SPACE CHARGE ALONG THE AXIS OF THE SECULAR REGION.

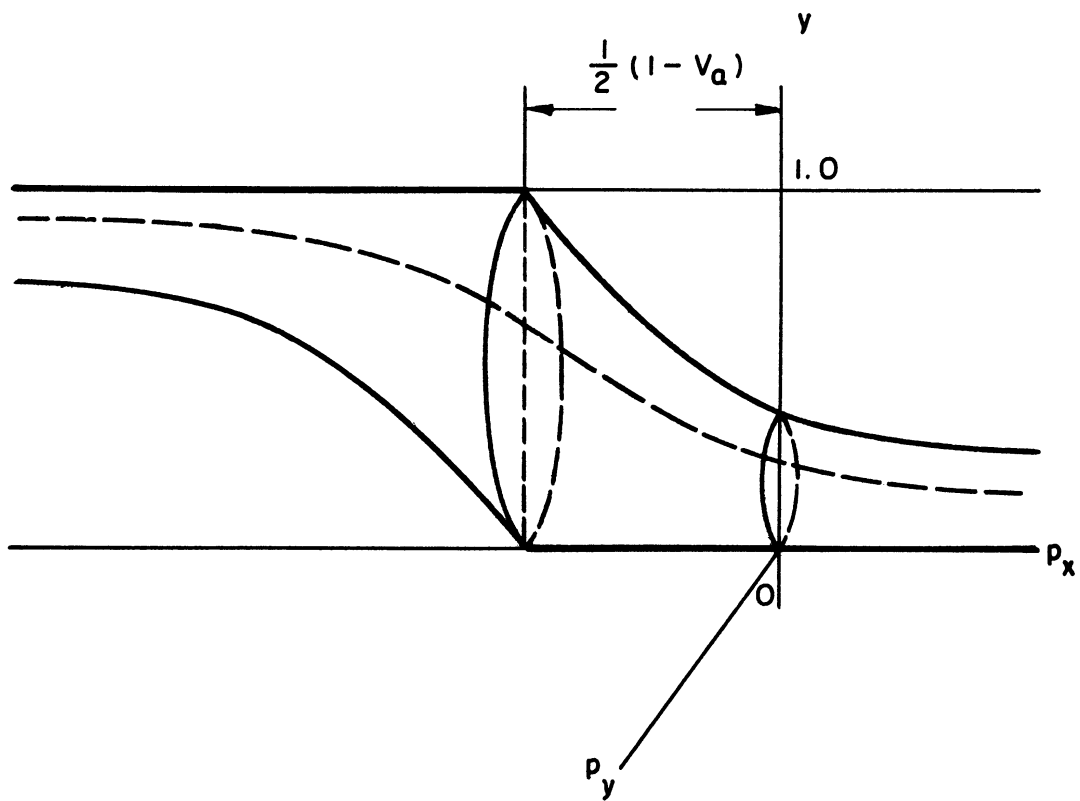


FIG. 5 SHAPE OF THE SECULAR REGION IN THE SECOND APPROXIMATION.

in the p_y -planes are no more circles; a closer analysis reveals that the axis of maximum density is displaced in the direction of the anode.

The boundary conditions at the source require an infinite number of modes corresponding to (21) and (24), the former type between the source and the base plane, the latter type to the right of the source and to the left of the base plane of the cone, but the fundamental modes have still the largest amplitude. Since the "flaring constant" n now varies with R , neither the Legendre function nor the radial function of (21) and (24) are applicable except as rough approximations.

IV. Confirmation and Conclusion

The justification for the semi-quantitative theory outlined above is the intuitive insight it gives in the formation and structure of the steady-state distribution rather than any accurate prediction of this distribution for given operating conditions. All the essential features of the theory are in very good agreement with measured data; from this fact we may infer that this intuitive insight is correct and useful.

I shall not here review all the available data. Peterson² proved beyond any reasonable doubt that the population in the secular region may be several times as large as that in the region accessible from the cathode. He also found very strong evidence for a double-stream condition in the cathode-accessible region, which is a necessary conclusion from the discussion of the second-order solution above, i.e., the formation of an annular source in this region. As a probe he employed a beam of electrons parallel to the axis of the magnetron. The most complete density data at the time of writing have been published by Nedderman,³ who collimated and measured the radiation from traces of gas excited by electron impact. This method gives excellent data except in the cathode region, where the electron energy is

too small (< 20 electron volts) to excite the gas particles. Figure 6 is a sample of Nedderman's data. His magnetron had anode and cathode radii of 0.36 and 0.22 inches, respectively. The dashed curve at the top of the graph is the Hull-Brillouin density at cutoff. The arrows indicate the edge of the cloud according to the Brillouin theory. It can easily be verified that the valley at the left is nearly entirely due to the omission of low-velocity electrons from the data. The most striking aspects of these data are the facts that the space-charge extends continuously from cathode to anode and that there is no conspicuous relation between the space-charge geometry and the "Hull radius."

Figure 7 has been replotted from Nedderman's data to show the dependence of the distribution on the magnetic field at nearly constant voltage. The decrease of the exponent γ_2 of $(d-y)$ close to the anode, as the cutoff condition is approached, is indicated by the curves, in agreement with the theory. The faintly curved line in this graph is the linear approximation (12) translated to cylindrical geometry.

According to the investigation presented above both theory and experiment indicate that already in the nonoscillating magnetron essentially the same radial charge distribution is established as prevails in the oscillating magnetron, the difference being primarily the variation with the azimuthal coordinate and the radial rate of flow. This is simply an extrapolation of the fact that the distribution calculated above is independent of the diffusion coefficient; the latter determines the current and the time required to reach a steady state but not the final charge distribution.

A small-signal theory established on the basis of a small perturbation on the Brillouin distribution suffers from the weakness that the whole space-charge configuration has to change radically, as soon as oscillations

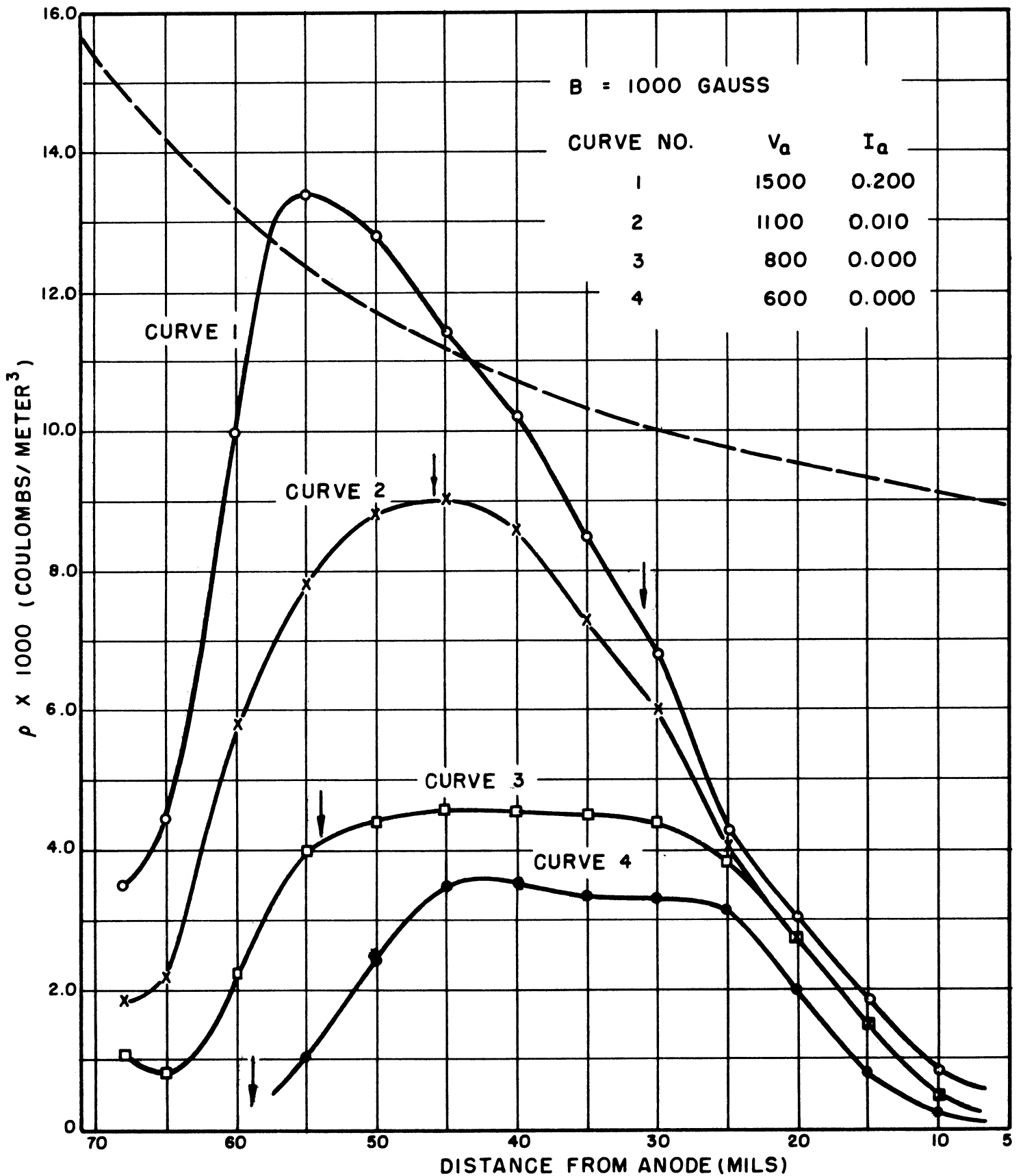


FIG. 6 OBSERVED DENSITY OF ELECTRONS OF MORE THAN 20 ELECTRON VOLTS ENERGY IN A STATIC MAGNETRON. (NEDDERMAN)

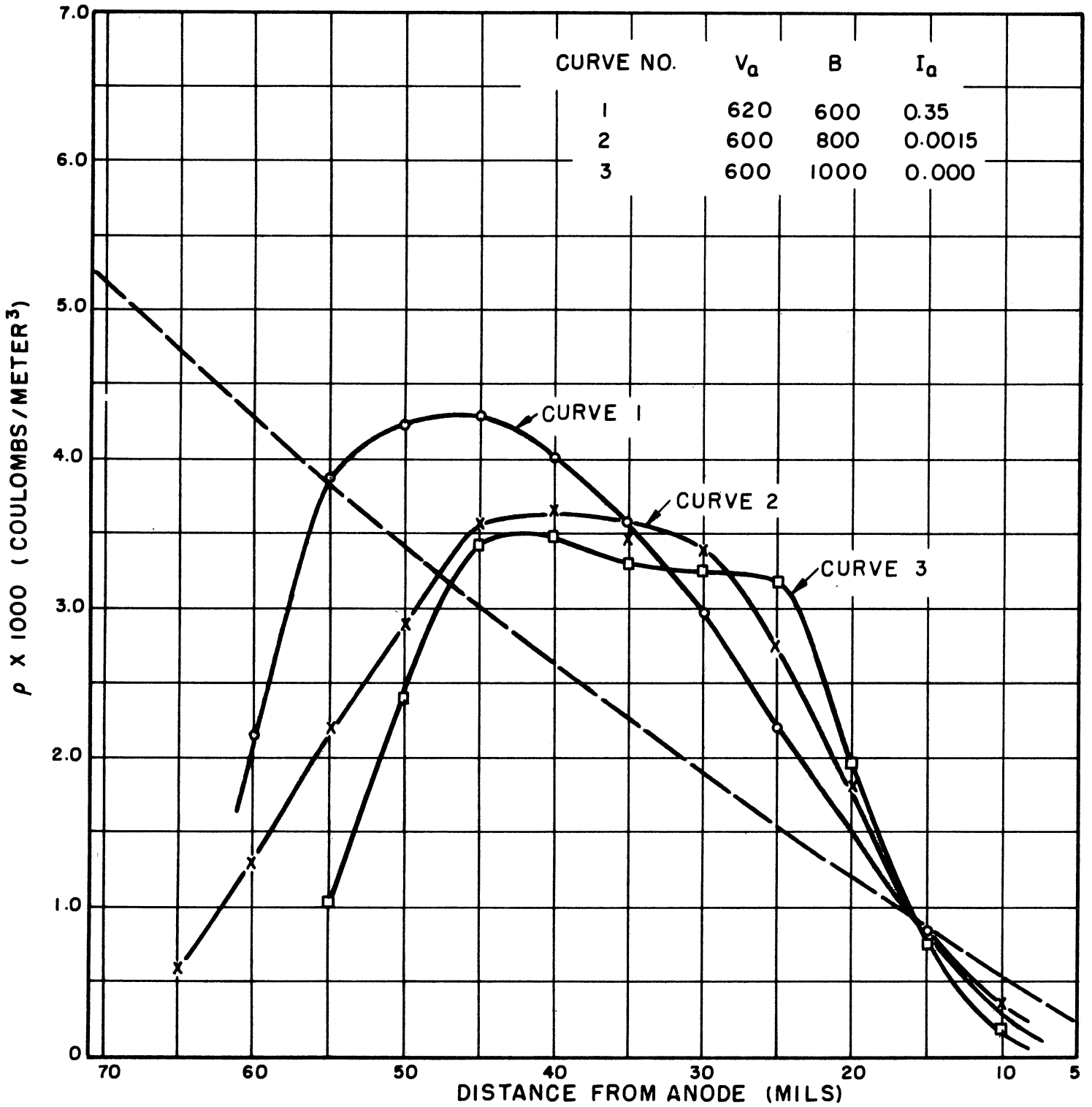


FIG. 7 COMPARISON OF NEDDERMAN'S RESULTS FOR DIFFERENT VALUES OF THE MAGNETIC FIELD.

start. In other words, there are two reasons for instability, the interaction of the electrons with the circuit, and the breakup of the Brillouin distribution. If the theory is based on an idealized laminar-flow steady-state such as the one presented in equations (12) and (13), on the other hand, these objections are overcome and an intuitively much more satisfactory foundation has been laid. Crude as this approximation may be, it is a significant improvement as a starting point for a small-signal theory of cw magnetrons.

The theory and the measurements confirming it also have some implications as far as the oscillating cw magnetron is concerned. An efficient magnetron oscillator operates far below the cutoff voltage; the oscillating state consequently originates from a space-charge distribution that outside the potential minimum is only a small fraction of the Brillouin density. The density can hardly be expected to increase essentially during oscillation. However, the reduced transit time and the increasingly organized flow of the electrons at larger amplitudes of oscillation make the statistical elements less important, so that more specific inferences as to the space-charge distribution become doubtful. In this light it may still be permissible to make the observation that no sharp border line is to be expected at small amplitude levels between a "hub" and the "spokes" of the revolving space-charge wheel in a cylindrical magnetron oscillator.

APPENDIX

CALCULATION OF THE DENSITY IN THE SECULAR REGION

With reference to Fig. 3 the first problem is to find the density in a given solid angle of a sphere. The current is assumed to be proportional to the density gradient only. The only source is at the origin, i.e., the apex of the right-hand cone.

$$\mathbf{J} = D \text{ grad } \rho \quad (27)$$

and

$$\text{div } \mathbf{J} = 0 \quad (28)$$

The second equation expresses continuity under steady-state conditions. Considering the fact that no variations occur with ϕ , the Laplacian in spherical coordinates is

$$\frac{1}{R^2} \frac{\partial}{\partial R} \left(R^2 \frac{\partial \rho}{\partial R} \right) + \frac{1}{R^2 \sin \theta} \frac{\partial}{\partial \theta} \left(\sin \theta \frac{\partial \rho}{\partial \theta} \right) = 0 \quad (29)$$

This equation must be corrected for the absence of diffusion in the y -dimension. Actually, neither the R -component, nor the θ -component of the isotropic flow (29) is orthogonal to the y -direction, but since the highest densities occur along the axis, which is orthogonal to y_1 in the modified geometry, we may on an approximate basis apply a correction to the θ -component only by multiplying the second term in (29) by one half; from symmetry each one of two Cartesian dimensions in a plane perpendicular to R accounts for exactly half the radial current in this plane. The lack of orthogonality between R and y_1 could be taken into account by means of another factor somewhat larger than one and dependent on the half-angle α of the cone.

The equation (29), modified by the first-mentioned correction factor, separates into the equations:

$$R^2 \frac{\partial^2 \rho_R}{\partial R^2} + 2R \frac{\partial \rho_R}{\partial R} - q^2 \rho_R = 0 \quad (30)$$

and

$$\frac{1}{\sin \theta} \frac{\partial}{\partial \theta} \left(\sin \theta \frac{\partial \rho_\theta}{\partial \theta} \right) + 2q^2 \rho_\theta = 0 \quad (31)$$

which have the solution given in equation (21) above. The separation constant q^2 satisfies the relations

$$\gamma^2 + \gamma - q^2 = 0 \quad (32)$$

and

$$n(n + 1) = 2q^2 \quad (33)$$

After the integration constants have been determined, (25) and (26), the y -variation of the fundamental diffusion mode is obtained by integration over the right and left halves of the secular region between the limits equivalent to y_1 and $y_1 + dy_1$.

$$\begin{aligned} \rho(y_1) dy_1 = & \int_{(y_1, dy_1)} \rho R^2 \sin \theta dR d\theta d\varphi \\ & + \int_{(y_1, dy_1)} \rho R_1^2 \sin \theta_1 dR_1 d\theta_1 d\varphi_1 \end{aligned} \quad (34)$$

where

$$y_1 = R(\cos \theta \cos \alpha + \sin \theta \cos \varphi \cos \alpha) \quad (35)$$

The most serious discrepancy between the resulting density distribution and the one assumed to begin with is the extremely rapid variation and high density obtained close to the potential minimum. The exponent γ_1 may have values down to about -1.6. As a basis for the discussion of the second-order secular region (Fig. 5), let us assume that the density varies inversely as the $3/2$ power of the distance from the singular point. For

physical reasons the density at the potential minimum is matched to this distribution a finite distance y_0 from the singularity. The "virtual" singularity thus falls at $y = -y_0$ outside the region under study. Integrating Poisson's equation with the obvious boundary conditions at $y = 0$, we obtain the potential in the vicinity of the minimum

$$V(y) = C \left\{ 2(y + y_0)^{1/2} - y \cdot y_0^{-1/2} - 2 y_0^{1/2} \right\} . \quad (36)$$

Consequently the boundary of the region accessible from the cathode in the $p_x y$ -plane is

$$p_x \geq C \left[\frac{(y + y_0)^{1/2} - y_0^{1/2}}{y} - \frac{1}{2} y_0^{-1/2} \right] - \frac{1}{2} y . \quad (37)$$

The corresponding boundary for anode-accessibility is

$$p_x \leq C \left[\frac{(y + y_0)^{1/2} - (\frac{1}{2} + y_0)y_0^{-1/2}}{y - 1} - \frac{1}{2} y_0^{-1/2} \right] - \frac{1}{2} (y + 1) . \quad (38)$$

These boundaries have the qualitative appearance shown in Fig. 5.

The axis of the secular region along which the density is largest can be found from the fact that p_y has its maximum for the value of y corresponding to this axis. For given p_x the equation of such an orbit is

$$(p_x + y)^2 + p_y^2 - V(y) = \text{const.} \quad (39)$$

Consequently

$$-2p_y \frac{\partial p_y}{\partial y} = 2(p_x + y) - \frac{\partial V}{\partial y} = 0 \quad (40)$$

or

$$p_x = \frac{1}{2} \frac{\partial V}{\partial y} - y . \quad (41)$$

This equation represents a line in the yp_x -plane, which is the axis of the secular region for a given potential distribution $V(y)$. We now want to compare the ordinates y_1 on this line with the ordinates y_2 on the line (7) representing the accessibility boundary:

$$p_x = \frac{1}{2} \frac{\partial V(y_1)}{\partial y} - y_1 = \frac{1}{2} \left(\frac{V(y_2)}{y_2} - y_2 \right) . \quad (42)$$

In these equations let us introduce the potential

$$V(y) = V_a \cdot y^p \quad (43)$$

and compute the ratio

$$\frac{y_2}{2y_1} = \frac{V_a^p y_1^{p-2} - 2}{2V_a y_2^{p-2} - 1} \quad \begin{cases} > 1 & \text{for } p > 2 \\ = 1 & p = 2 \\ < 1 & p < 2 \end{cases} \quad (44)$$

The inequalities are found by small variations from the condition $p = 2$, which represents the circular orbits used in the first-order calculations above.

In the first-order sample shown in Fig. 4 the discontinuity in the derivative always occurs at $y = 1/2$ because of the circular orbits assumed. In Fig. 7, on the other hand, the rapid change in slope happens closer to the anode, particularly far from cutoff, i.e., where the exponent differs the most from 2, in good agreement with the second-order theory.

LIST OF REFERENCES

1. Hok, G., "A Statistical Approach to the Space-Charge Distribution in a Cut-off Magnetron", Jour. App. Phys., 23, 983-989 (September, 1952).
2. Peterson, W. W., "The Trajectron--An Experimental DC Magnetron", Tech. Rpt. No. 18 and dissertation for a Ph. D. degree, Electron Tube Laboratory, Dept. of Elec. Eng., The University of Michigan, May, 1954.
3. Nedderman, H. C., "Space-Charge Distribution in a Static Magnetron", Jour. App. Phys., 26, 1420-1430 (December, 1955).

DISTRIBUTION LIST

<u>No. Copies</u>	<u>Agency</u>
3	Project Engineer, Microwave Tube Branch, Evans Signal Laboratory, Belmar, New Jersey
1	Mail and Records, Evans Signal Laboratory, Belmar, New Jersey
1	Technical Documents Center, Evans Signal Laboratory, Belmar, New Jersey
1	Director of Research, Hexagon, Fort Monmouth, New Jersey
1	Electronics Research Laboratory, Stanford University, Stanford, California, Attention: Applied Electronics Laboratory, Document Library
1	The Director, U. S. Naval Research Laboratory, Code 2021, Washington 25, D. C.
1	Commander, Air Force Cambridge Research Center, CROOIR-2E, L. G. Hanscom Field, Bedford, Massachusetts
1	Commander, Rome Air Development Center, Electronic Development Division, RCSSTL-1, Griffis Air Force Base, New York
1	Chief Signal Officer, Department of the Army, Washington 25, D. C., Attention: SIGRD
1	Advisory Group on Electron Tubes, 346 Broadway, New York 13, New York
5	Armed Services Technical Information Agency, Document Service Center, Knott Building, Dayton 2, Ohio
2	Commander, Wright Air Development Center, WCOSI-3, Wright-Patterson Air Force Base, Ohio
1	Commanding Officer, U. S. Army Signal Electronics Research Unit, Mountain View, California
1	Chief of Ordnance, Washington 25, D. C., Attention: ORDTX-AR
1	Commanding General, Redstone Arsenal, Huntsville, Alabama, Attention: Technical Library
1	Commanding Officer, Watertown Arsenal, Watertown, Massachusetts, Attention: OMRO
1	Commanding Officer, Frankford Arsenal, Philadelphia 37, Pennsylvania, Attention: ORDBA-FEL

No. CopiesAgency

1 Chief, Bureau of Ships, Department of the Navy, Washington 25, D. C.
Attention: Code 816A

1 Commander, Wright Air Development Center, WCRET-3, Wright-Patterson
Air Force Base, Ohio

1 Chief, Ordnance Corps, Department of the Army, Diamond Ordnance Fuze
Laboratories, Connecticut Avenue and Van Ness Street, N.W., Washing-
ton 25, D. C., Attention: T. T. Liimatainen

1 Commanding General, U. S. Army Electronic Proving Ground, Fort Hua-
chuca, Arizona, Attention: EWD (Technical Library)

1 Commanding General, Aberdeen Proving Ground, Aberdeen, Maryland,
Attention: Development and Proof Service, Fire Control Division,
Capt. Alter

1 Chief, Radar Development Branch, Radar Division, Surveillance Dept.,
USASEL, Evans Area, Belmar, New Jersey

1 General Electric Company, 1 River Road, Schenectady 5, New York,
Attention: Dr. E. D. MacArthur

1 Raytheon Manufacturing Company, Foundry Avenue, Waltham 54, Massachu-
setts, Attention: W. T. Welsh

1 Varian Associates, 611 Hansen Way, Palo Alto, California, Attention:
Mrs. Helen Dean, Technical Library

1 Litton Industries, East Brittan Avenue, San Carlos, California, Attention:
Dr. N. Moore

1 Sylvania Electric Products, Inc., 100 Sylvan Road, Woburn, Massachusetts,
Attention: Mr. M. Pease

1 Director, National Bureau of Standards, Boulder, Colorado, Attention:
Radio Library

1 Director, Countermeasures Division, Evans Signal Laboratory, Belmar,
New Jersey

1 Director, Evans Signal Laboratory, Belmar, New Jersey, Attention: Mrs.
Betty Kennett, Report Distribution Unit, Electron Devices Division

11 Director, Evans Signal Laboratory, Belmar, New Jersey, Attention: Mr.
Gerald Pokorney, Microwave Tubes Branch, Electron Devices Division

1 Sylvania Electric Products, Inc., Microwave Tube Laboratory, Mountain
View, California, Attention: Dr. D. Goodman

1 Sylvania Electric Products, Inc., Physics Laboratories, Bayside 60,
Long Island, New York, Attention: Dr. R. G. E. Hutter

No. Copies

Agency

- 1 Prof. Jules S. Needle, Electrical Engineering Department, Northwestern University, Evanston, Illinois
- 1 Bendix Aviation Laboratories, Northwestern Highway and 10 1/2 Mile Road, Detroit 35, Michigan, Attention: Dr. J. H. Bryant
- 1 General Electric Microwave Laboratory, Palo Alto, California, Attention: Dr. E. Nalos
- 1 California Institute of Technology, Pasadena, California, Attention: Dr. R. Gould, Electrical Engineering Department
- 1 Commanding Officer, U. S. Signal Support Agency, Fort Monmouth, New Jersey, Attention: SIGRM/ES-ASA
- 1 Electronics Research Laboratories, Stanford University, Stanford, California, Attention: Dr. M. Hare and Mr. Dould
- 1 Engineering Research Institute, Project Files, 132A Cooley Building North Campus, The University of Michigan, Ann Arbor, Michigan